IET Microwaves, Antennas & Propagation

Research Article

IET Journals
The Institution of Engineering and Technology

Planar meandered-F-shaped 4-element reconfigurable multiple-input–multiple-output antenna system with isolation enhancement for cognitive radio platforms

ISSN 1751-8725
Received on 25th February 2015
Revised on 25th July 2015
Accepted on 30th September 2015
doi: 10.1049/iet-map.2015.0139
www.ietdl.org

Rifaqat Hussain ✉, *Mohammad S. Sharawi*

Electrical Engineering Department, King Fahd University of Petroleum and Minerals (KFUPM), Dhahran 31261, Saudi Arabia
✉ *E-mail: rifaqat@kfupm.edu.sa*

Abstract: In this study, a novel meandered reconfigurable F-shaped antenna is presented. The proposed design is a 4-element, dual mode, multiple-input–multiple-output (MIMO) antenna system. Frequency agility is achieved using P-type intrinsic N-type (PIN) diode switching while frequency tuning is realised using varactor diodes. The proposed design covers wide frequency bands below 1 GHz and is realised on a single substrate. The proposed design is compact and highly suitable to be used in cognitive radio-based wireless handheld devices. An isolation enhancement technique is applied to reduce the mutual coupling between various MIMO elements. Rectangular defected ground (GND) slots are used to reduce the mutual coupling between horizontally placed antenna elements while staircase type GND plane structure is introduced to enhance the isolation between vertically placed antenna elements. The antenna elements are also evaluated for MIMO performance metrics. The antenna system covers a size of $65 \times 120 \times 1.56$ mm^3.

1 Introduction

Wireless communication systems have evolved considerably over the past ten years. The proliferation of wireless handheld devices such as smart phones and tablet personal computer's may result in ten-fold data rate demands in the next few years. The rapid growth of wireless devices results in an increasing demand of wireless services and hence high data rate. Thus, it becomes necessary to improve the wireless system capacity to enhance its throughput. This can be made possible by using wide bandwidth operation, improved spectral efficiency and incorporating cognitive radio (CR) techniques using multiple-input–multiple-output (MIMO) systems. The CR is an efficient technique of spectrum utilisation.

A CR-based system dynamically interacts with the radio-frequency (RF) environment to sense the unoccupied or under-utilised frequency bands and hence changes the operating band by switching to another frequency. Reconfigurable MIMO antenna systems are of great importance for the realisation of CR platforms. Frequency reconfigurable antennas for CR platforms have attracted researchers over the past few years. Single element reconfigurable antennas or MIMO reconfigurable antennas can be used in CR applications. Several works were reported using single element reconfigurable antennas for CR applications [1–3]. In [1], a frequency reconfigurable communication antenna was proposed for CR platforms. The frequency band covered was 1.6–2.6 GHz with total substrate area of 30×41 mm^2. A frequency reconfigurable printed Yagi-Uda dipole antenna was presented in [2] for CR applications. The frequency band covered was 400–750 MHz with total substrate area of 745×360 mm^2. The proposed antenna is a good candidate for low-frequency bands of operation in CR platforms. However, the total substrate area is formidable to be used in small wireless handheld devices. A non-planar reconfigurable antenna was presented in [3] with a ground (GND) plane dimensions of 400 mm × 400 mm. The proposed design was very versatile as it covered several frequency bands including 800–900 MHz, 1.7–2.5 GHz, 3–3.6 GHz and 5.1–5.9 GHz. Though the design covered low-frequency bands along with other several bands, the non-planar structure with large board dimensions makes it unsuitable to be used in mobile terminals and other wireless handheld devices.

Reconfigurable antennas with MIMO capabilities are highly desirable in CR platforms. It could be utilised to enhance the capacity along with data reliability as well. Several MIMO reconfigurable antenna designs were reported in the literature for CR applications [4–6]. In [4], a 2-element reconfigurable MIMO design was presented. The MIMO antenna system was a combination of balanced dipole and a two-port chassis antenna. The single arm length of the dipole was 70 + 40 mm with track width of 1 mm while the chassis antenna was with a total area of 118×40 mm^2. The height of the antenna was 7 mm. Varactor diode-based reconfigurable antennas were operating with an applied voltage up to 15 V. The frequency bands covered were 646–848 MHz. The non-planar elevated antenna structure with large varactor biasing voltage made this an inappropriate choice to be used in wireless handheld devices. In addition, it did not provide any quantitative analysis of the MIMO performance of the proposed antennas.

In [5], a 2-element MIMO reconfigurable design was presented. The proposed design was an elevated printed inverted F-shaped antenna (PIFA) with single element dimensions of $10 \times 10 \times 6.4$ mm^3. The frequency bands covered were 2.3–2.4 GHz, 2.5–2.7 GHz and 3.4–3.6 GHz. Similarly, a PIFA-based MIMO antenna was proposed in [6], with frequency bands 2.1–2.9 GHz and single element dimensions of $16 \times 33 \times 5$ mm^3. The designs provided in [5, 6] were elevated PIFA structures, covering high-frequency bands above 2 GHz and hence are not suitable candidates for low-frequency mobile standards and wireless handheld devices. A 4-element PIFA-based MIMO was presented in [7] covering frequency bands from 2.4 to 2.8 GHz with single element dimensions of $30 \times 30 \times 16.4$ mm^3 on GND plane dimensions of 120×120 mm^2. This design is not compact with a large GND plane and thus inappropriate to be used in compact wireless handheld devices. In [8], a low-frequency 2-element MIMO antenna system was presented for CR applications. It utilised PIN and varactor diodes for frequency reconfigurability and provided two modes with single element size of 7.6×56.6 mm^2. Isolation enhancement techniques were investigated and used to

reduce the mutual coupling between antenna elements. In addition, it did not provide any channel capacity calculation to validate the MIMO operation. Moreover, four antenna elements cannot be accommodated within the given board dimensions.

In this paper, a reconfigurable single substrate-based 4-element planar MIMO antenna system is presented for CR applications. The proposed design can be utilised as a communication antenna or aids in the search of available bands via specialised band switching for spectrum sensing CR platforms. The single antenna element is a unique combination of meandered modified inverted F-shaped antenna (IFA) like structure. Each antenna element is integrated with PIN diodes to switch over the major band regions, whereas varactor diodes are used to sweep within the major frequency bands (fine tuning). The distinguishing feature of the proposed design is that it accommodates 4-element reconfigurable MIMO antennas on a substrate area of that of a typical smart phone size. The planar structure and its operation at lower-frequency bands below 1 GHz are the key features of the proposed design. Planar low-profile reconfigurable antennas designs found in the literature for CR applications with comparable sizes to the proposed design covered frequency bands above 2 GHz [9–11].

Moreover, the high mutual coupling within closely spaced antenna elements was mitigated using a novel approach to enhance the isolation. Rectangular slots were created between horizontally placed antenna elements to improve the isolation between them. A better isolation between vertically placed antenna elements was achieved by optimising the shape of the GND plane. The complete MIMO antenna systems are developed on single board of dimensions $65 \times 120 \times 1.56$ mm^3 with single element dimensions consisting of the sum of 7.9×37 mm^2 and 17.7×19.6 mm^2. Additionally, a systematic design procedure is detailed which might be helpful to design multi-element planar MIMO antennas for any desired band with compact size. The proposed design is investigated for MIMO parameters including channel capacity calculation.

2 Design details

2.1 4-element MIMO antenna design details

First, the 4-element reconfigurable meandered line IFA MIMO antenna is presented in Figs. 1*a* and *b*. A 4-element MIMO antenna system is fabricated on a single substrate board with dimensions $65 \times 120 \times 1.56$ mm^3. The design was fabricated on Rogers 4003 substrate with $\varepsilon_r = 3.55$. The four antenna elements are printed on the top layer of the board, whereas the bottom layer has the GND plane.

An IFA is a horizontal monopole that is parallel to the GND plane. An IFA is roughly $\lambda/4$ antenna with its feeding point coming from the GND plane. The arm of the IFA is short circuited to the GND plane to cancel the capacitive effect at its input. Thus, the structure formed by this configuration resembles the letter inverted F and hence it is called an IFA [12].

The design procedure of the single element structure was started with the well-known IFA. The antenna was resonating at frequency band above 2 GHz. To bring the resonance frequency to lower bands, extra meander lines were added to the antenna structure. The design was optimised using high-frequency structure simulator (HFSS). Parametric sweeps were conducted for the length and placement of the shorting wall and optimised to bring down the resonating frequencies below 1 GHz. In addition, two slots were created in the solid structure to add the capacitive effect which achieves reconfigurability in the proposed architecture by varying the capacitance.

The given antenna operates in two modes. The length corresponding to mode-1 and mode-2 operations are approximately equal to $\lambda/12$. The given antenna structure is embedded with a DC blocking capacitor, PIN diode and varactor diode in series with the radiating branch of the antenna. The given design is provided with a shorting wall of length 7.9 mm instead of 1.48 mm single shorting strip. The reactive impedances added to the radiating structure further reduce the length of the antenna and resonance occurred at lower bands.

A detailed view of the 2-element MIMO antenna is shown in Fig. 2. Fig. 2*a* shows the top view of the two out of four similar antenna structures, whereas side view of the proposed design is shown in Fig. 2*b*. PIN diodes were used for coarse mode selection, whereas varactor diodes were utilised for smooth variation of the resonating frequencies. The fine tuning of the varactor is more notable in lower-frequency bands.

The biasing circuitry for the two diodes is shown in Fig. 3. The same biasing circuitry was used by the same diodes. The biasing circuit is practically isolated from the radiating structure using an RF choke while the DC blocking capacitor prevents flow of DC current into the radiating branches. The varactor diode is reverse biased all the time, whereas the PIN diode is used for switching

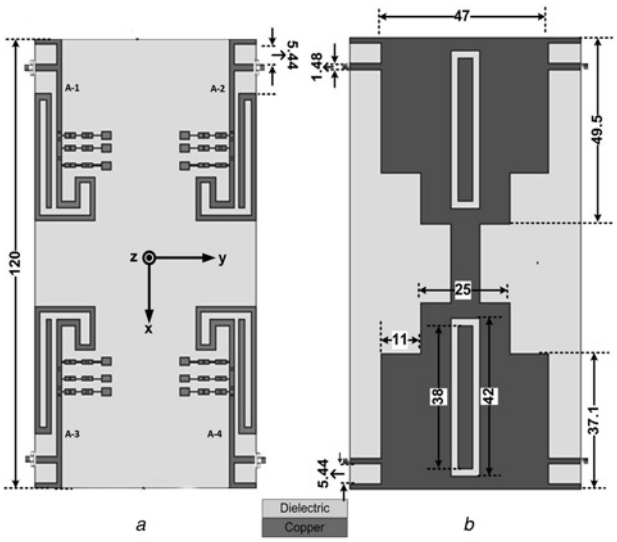

Fig. 1 *Proposed four elements MIMO antennas system for CR platform*
a Top view
b Bottom view – all dimensions are in millimetres (mm)

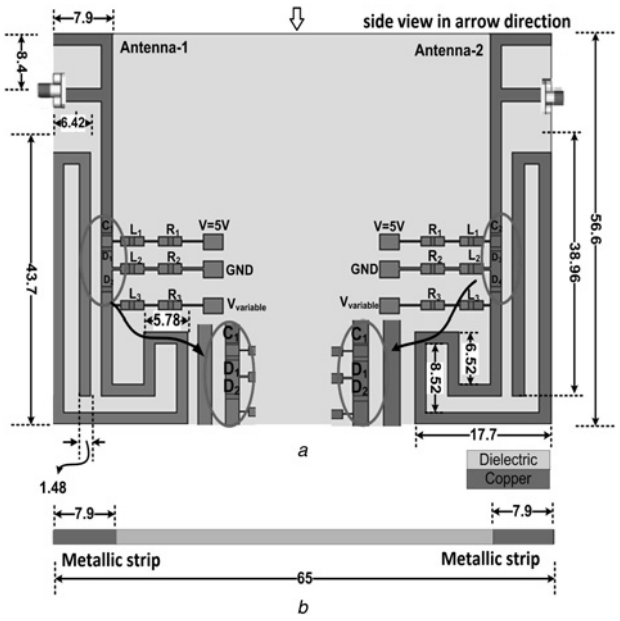

Fig. 2 *Detailed schematic of the 2-element reconfigurable MIMO antenna*
a Top view
b Side view – all dimensions are in mm

IET Microw. Antennas Propag., 2016, Vol. 10, Iss. 1, pp. 45–52

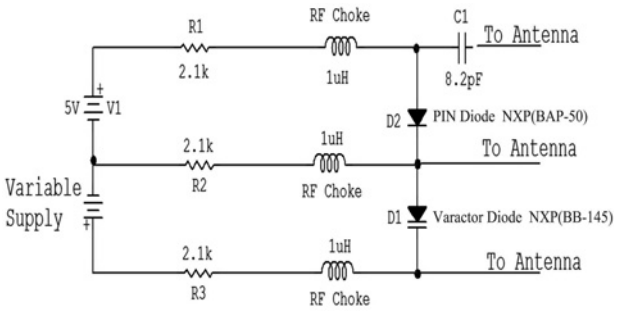

Fig. 3 *PIN and varactor diodes biasing circuitry*

purposes (ON/OFF). The values used for RF choke and resistor were 1 μH and 2.1 kΩ, respectively.

The fabricated model is shown in Fig. 4. Fig. 4*a* shows the top view of fabricated model, whereas Fig. 4*b* shows the GND plane of the fabricated design.

2.2 Isolation enhancement

In MIMO systems, various antenna elements are integrated within mobile and other small wireless handheld devices to increase the throughput.

However, poor isolation can affect the overall efficiency and diversity performance. It is necessary for good MIMO performance that antennas are well isolated especially at lower-frequency bands. The high mutual coupling within closely spaced antenna elements, as shown in Fig. 1, were mitigated using a novel approach for enhancing the isolation. The antenna elements given in Fig. 1 are optimised to be placed in a standard smart phone size. This results in high mutual coupling between antenna elements placed horizontally and vertically. Rectangular slots were created between horizontally placed elements to improve the isolation between them. However, it had negligible effects on the vertically placed antenna elements. Better isolation was achieved between vertically placed antenna elements by optimising the shape of the GND plane.

Both defected ground structures (DGS) increase the current paths in the GND plane thus minimising the port coupling between close antenna structures. The DGS loop also acts as a band select filter when its dimensions are designed properly. Parametric studies were conducted to optimise the DGS sizes for the bands of interest.

3 Simulation and measurement results

The optimised reconfigurable MIMO antenna with enhanced isolation was fabricated and scattering parameters were measured using an Agilent N9918A vector network analyser. The details of the two covered modes are as follows.

3.1 Mode-1

In mode-1, the PIN diodes are switched OFF, whereas the varactor diodes are reverse biased. The reverse bias voltage is varied between 0 and 6 V. For mode-1, the effect of capacitance variation on the radiating structure is minimal and hence on the resonance frequency as well. The resulted simulated and measured reflection coefficients of mode-1 are shown in Fig. 5. In mode-1, the bands covered are 1170 and 2420 MHz with a −6 dB operating bandwidth of at least 100 MHz in both bands.

3.2 Mode-2

In this mode, the PIN diodes are switched ON and varactor diodes reverse bias voltage was varied between 0 and 6 V. In this mode, varactor diodes have a significant effect on the resonating frequencies. The resonating frequency was smoothly changed at the lower-frequency band below 1 GHz. A significant bandwidth is achieved at the lower bands while the addition of a reactive impedance has insignificant effects on higher-frequency band. The first resonating frequency was varied between 743 and 1030 MHz,

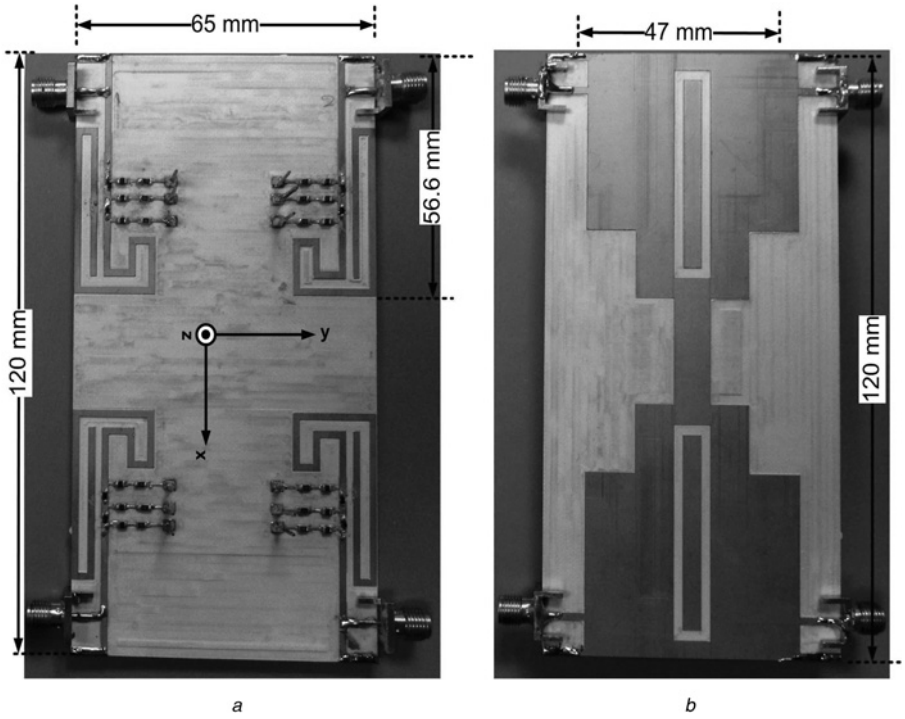

Fig. 4 *Fabricated model*

a Top view
b Bottom view showing the reference GND plane

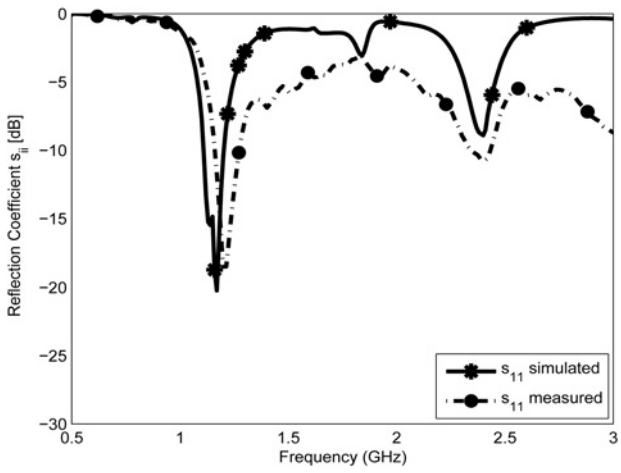

Fig. 5 *Reflection coefficients of the MIMO antenna system – mode-1*

whereas the second band covered was relatively constant at 2400 MHz. The minimum −6 dB operating bandwidths for the two bands were 60 MHz and 120 MHz. The simulated reflection coefficients are shown in Fig. 6*a* for mode-2, whereas measured reflection coefficients are shown in Fig. 6*b*.

The diode can be modelled as variable capacitor in HFSS. The various capacitance values correspond to the capacitance of the actual varactor diode when biased properly. Losses were taken into account while modelling the lumped element in HFSS as per the data sheet. The legend used for simulated reflection coefficient curves corresponds to different capacitance values of the varactor diode and hence are represented in picofarad. In the fabricated model, the resonating frequency is varied by applying reverse bias voltage across varactor diode. Different voltage levels correspond to different capacitance values of the varactor diode. The legend used for the measured reflection coefficient curves are actually the different bias voltages applied across varactor diode and hence it is represented in volts.

The simulated and measured reflection coefficient curves in Figs. 5 and 6 show close agreement. The slight difference in frequency can be

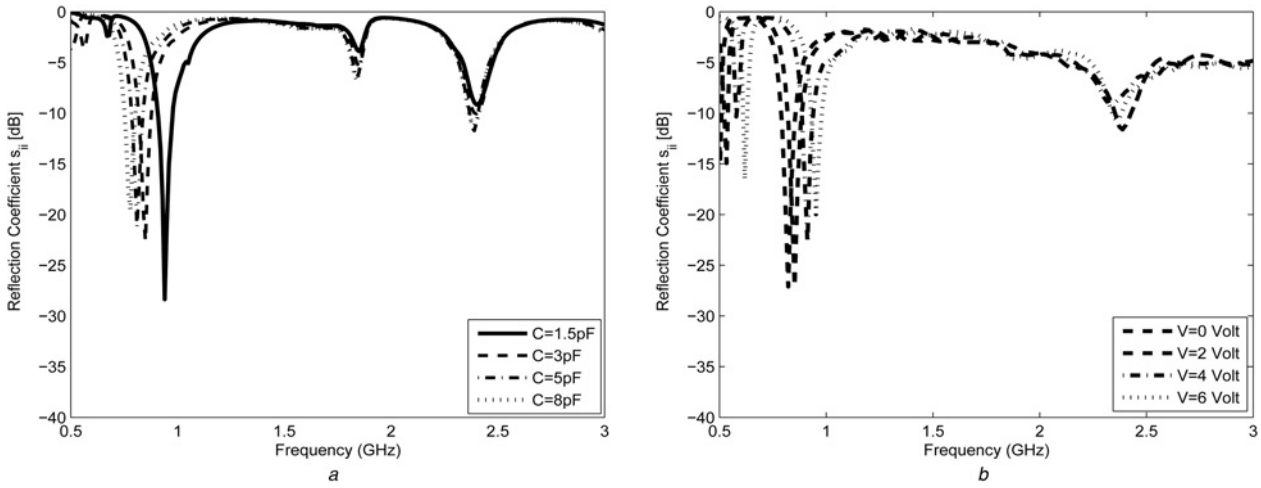

Fig. 6 *Reflection coefficients of the MIMO antenna system – mode-2*

a Simulated curves
b Measured curves

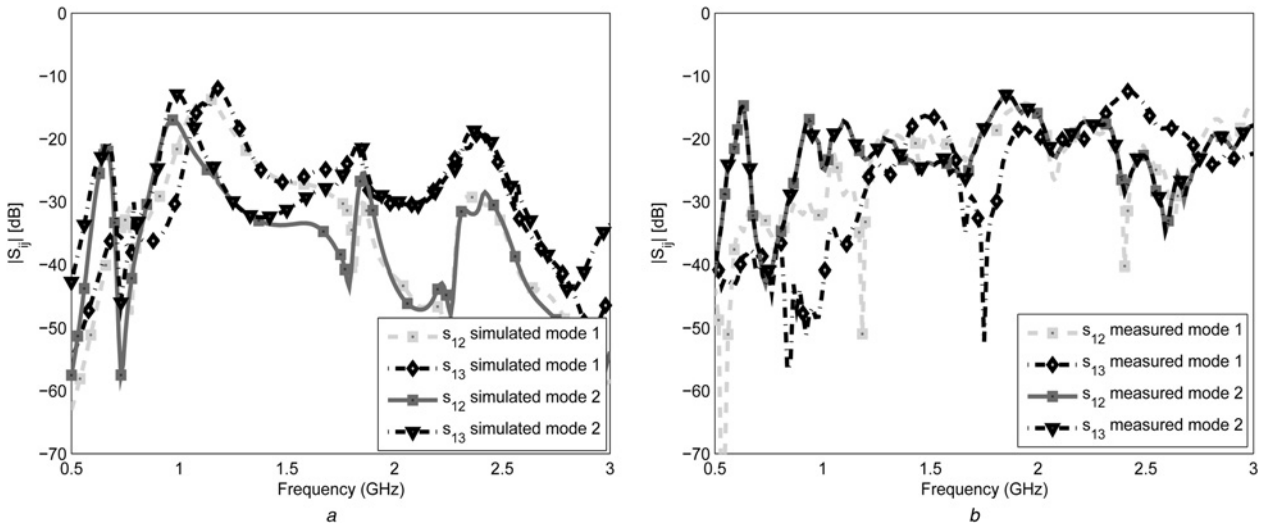

Fig. 7 *Transmission coefficient curves between MIMO antenna elements*

a Simulated
b Measured

IET Microw. Antennas Propag., 2016, Vol. 10, Iss. 1, pp. 45–52

caused by substrate properties and fabrication tolerances. Moreover, PIN and varactor diodes were modelled according to the data provided by their data sheets. The lack of flexibility of modelling in HFSS might be the cause of the minor frequency shift as well. The PIN diodes were modelled as resistive and capacitive circuits in forward and reverse bias conditions, respectively, whereas the varactor diode was modelled as a variable capacitor.

3.3 Isolation enhancement results

The closely spaced antenna elements in MIMO configuration require good isolation in mobile and other small wireless handheld devices. In the current design, rectangular slots and modified GND plane structure are used to enhance the isolation between all antenna elements.

Isolation is a measure of power coupled between various antenna elements in a multi-antenna system. Isolation is equal to $|S_{ij}|$ where S_{ij} is the magnitude of the transmission coefficient. The simulated and measured isolation curves after incorporating the isolation enhancement methods are shown in Figs. 7*a* and *b*, respectively. The curves show the isolation between antenna elements (A-1, A-2) and (A-1, A-3). The worst-case simulated and measured isolation values were 12.5 and 12 dB between the MIMO antenna elements across all the operating bands. The isolation enhancement structure improved the isolation by at least 3 dB when compared with a similar MIMO antenna without the isolation enhancement method used in this paper.

3.4 Far-field radiation characteristics

The simulated 3D gain patterns for antenna elements for mode-1 at 1160 MHz are shown in Fig. 8. The maximas of the gain patterns for each element are tilted with respect to its adjacent elements, thus resulting in lower-field correlation. The radiation patterns were measured at Microwave Vision, Italy, using a Société d'Applications Technologiques de l'Imagerie Micro-Onde (SATIMO) Starlab anechoic chamber. The measuring setup is shown in Fig. 9. The simulated and measured peak gains for mode-1 were (−0.77 dB, 3.52 dB) and (−3.64 dB, 3.51 dB), for the two bands at 1170 and 2420 MHz, respectively. While for mode-2, the values were (−1.8 dB, 3.52 dB) and (−2.18 dB, 3.44 dB), for the two bands at 950 and 2400 MHz, respectively. The simulated and measured peak gains are for a single antenna element and are given in decibels.

The efficiencies (η %) for mode-1 at two bands were (52, 78), respectively, whereas for mode-2, the values for two bands were

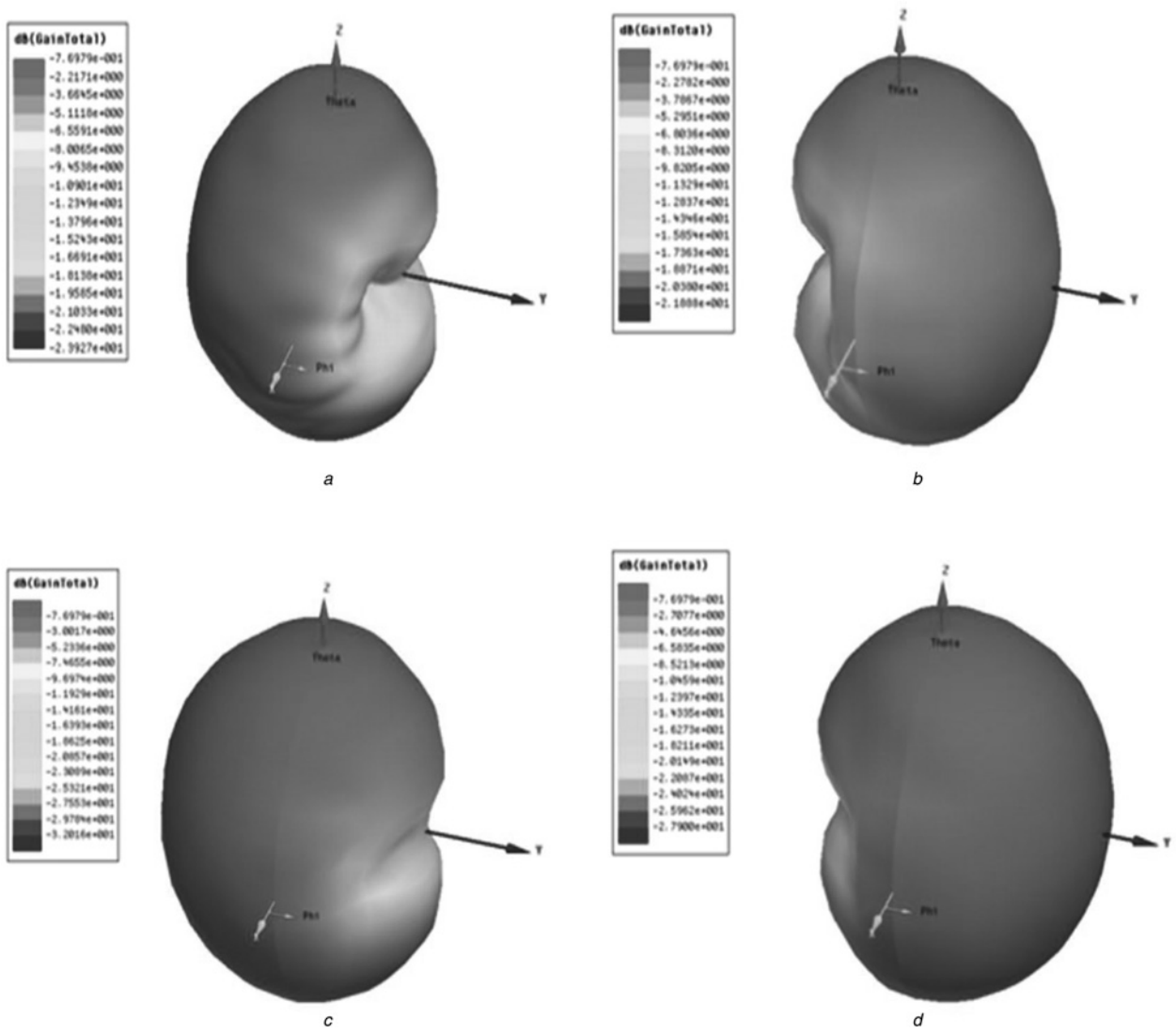

Fig. 8 *Simulated 3D gain pattern mode-1*

a Antenna-1 excited at 1160 MHz
b Antenna-2 excited at 1160 MHz
c Antenna-3 excited at 1160 MHz
d Antenna-4 excited at 1160 MHz

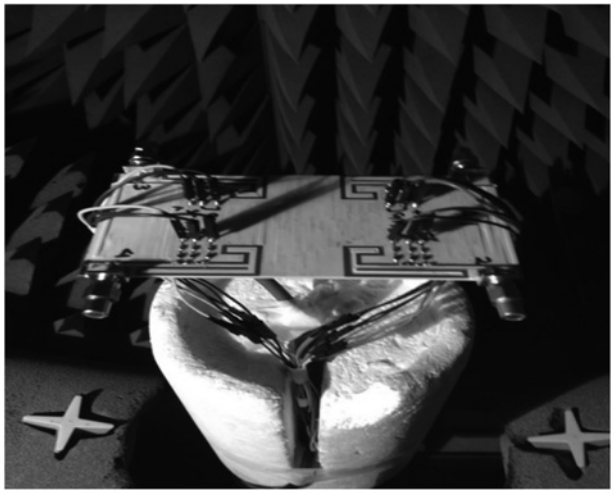

Fig. 9 *Radiation pattern measurement setup*

(34, 78). The low efficiency of mode-2 at the lower band is because of the electrically small antenna nature of the proposed design.

The two-dimensional (2D) measured radiation patterns of the given antenna are shown in Figs. 10 and 11 for antenna elements 1 and 2 (3 and 4 are identical). Fig. 10 shows the normalised measured radiation patterns of the proposed MIMO antenna system at 2400 MHz of mode-1. All co-pol and cross-pol patterns for the two elements of the MIMO antenna are given in Figs. 10*a* and *b* for the *xz* and *yz* planes, respectively. Fig. 11 shows the measured gain pattern at 950 MHz of mode-2. All co-pol and cross-pol patterns are given in Figs. 11*a* and *b* for the *xz* and *yz* planes, respectively. The *xz* and *yz* planes are referred to antenna orientation as shown in Fig. 1.

3.5 Envelope correlation coefficient

The correlation coefficient (ρ) is an important parameter for MIMO performance metrics evaluation. It is a measure of isolation or correlation between different MIMO channels. This metric considers the radiation pattern of the antenna system and its effect

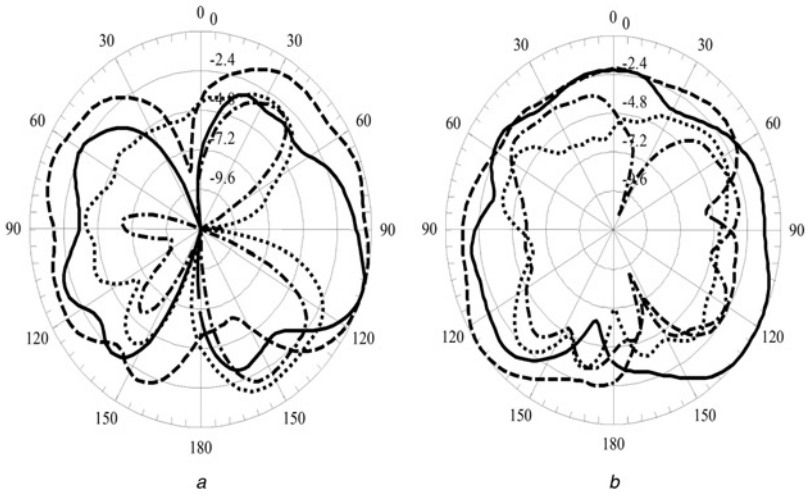

Fig. 10 *Measured normalised radiation patterns for the proposed MIMO antenna mode-1*

a *xz*-plane at 2400 MHz
b *yz*-plane at 2400 MHz
Solid: co-pol element 1; dashes: co-pol element 2; dotted: cross-pol element 1; and dashes-dot: cross-pol element 2

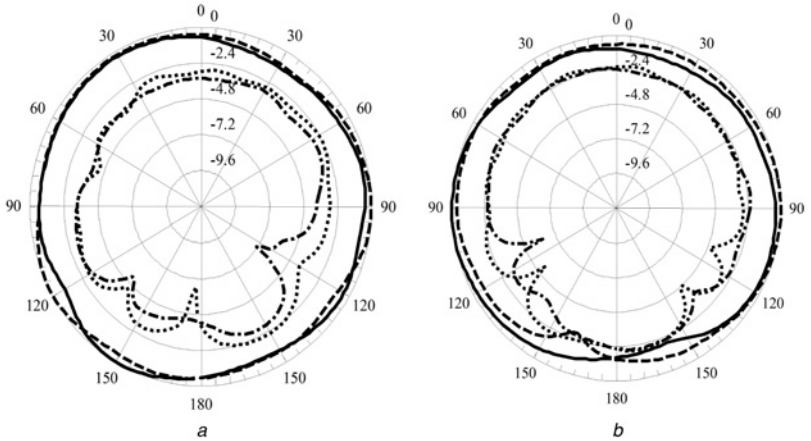

Fig. 11 *Measured normalised radiation patterns for the proposed MIMO antenna mode-2*

a *xz*-plane at 950 MHz
b *yz*-plane at 950 MHz
Solid: co-pol element 1; dashes: co-pol element 2; dotted: cross-pol element 1; and dashes-dot: cross-pol element 2

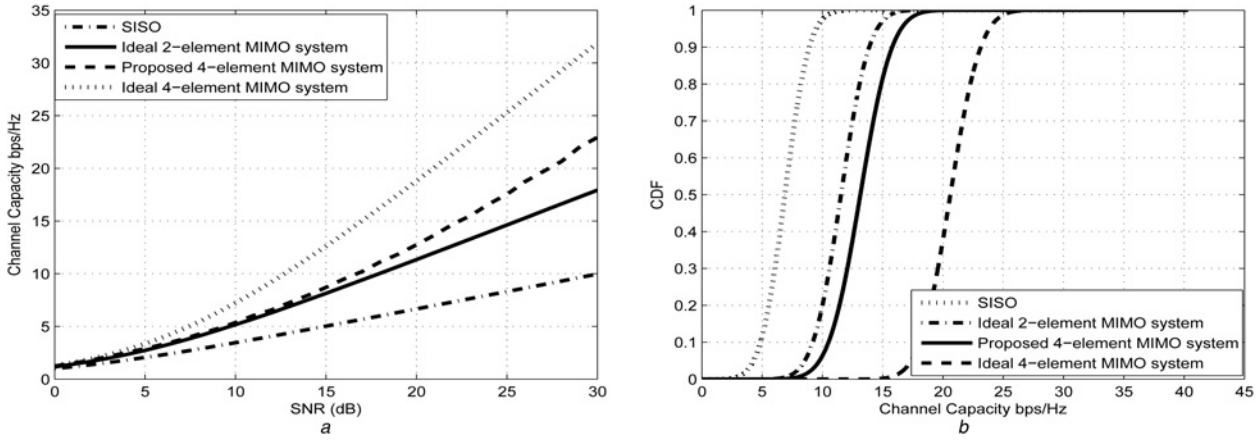

Fig. 12 *Channel capacity is calculated for the proposed design at mode-2 at 950 MHz*

a Average channel capacity in urban mobile environment – mode-2 at 950 MHz
b CDF of channel capacity – mode-2 at 950 MHz

on one another when operated simultaneously (which is the case in a MIMO antenna system). The envelope correlation coefficient (ρ_e) can be calculated using the following formula [13]

$$\rho_e = \frac{\left|\iint_{4\pi}[\boldsymbol{F}_i(\theta,\ \varphi) * \boldsymbol{F}_j(\theta,\ \varphi)]\,\mathrm{d}\Omega\right|^2}{\iint_{4\pi}\left|\boldsymbol{F}_i(\theta,\ \varphi)\right|^2\mathrm{d}\Omega \iint_{4\pi}\left|\boldsymbol{F}_j(\theta,\ \varphi)\right|^2\mathrm{d}\Omega} \tag{1}$$

where $\boldsymbol{F}_i(\theta, \varphi)$ is the field radiation pattern of the antenna when ports i, j are excited and * denotes the Hermitian product. The ρ_e were calculated using the measured radiation patterns. The measured 3D patterns for mode-1 at the two covered bands are 0.018 and 0.083, whereas for mode-2, the values at the two bands were 0.021 and 0.123. respectively.

3.6 Channel capacity calculation

The basic purpose of MIMO antenna systems in fourth generation wireless standards is to increase the throughput in multi-path and fading environments. The channel capacity calculation/measurement depends greatly on the correlation among various antennas patterns and types of propagation channels. For better channel capacity, high isolation and low correlation are desirable among the antennas elements. The capacity of an $N \times N$ MIMO antenna system is given as [14]

$$C = \log_2\left(\det\left[\boldsymbol{I} + \frac{\mathrm{SNR}}{N}\boldsymbol{H}H^*\right]\right) \tag{2}$$

where C is the channel capacity, $\boldsymbol{I}$ is the $N \times N$ identity matrix, $\boldsymbol{H}$ is the channel coefficient matrix and H^* is the conjugate transpose of $\boldsymbol{H}$ and SNR is the signal-to-noise ratio. The matrix $\boldsymbol{H}$ contains the information about the propagation channel between the transmitting and receiving antennas.

In this section, channel capacity is calculated using the 2D measured radiation patterns for the proposed 4-element MIMO antenna system and a theoretical channel coefficient matrix ($\boldsymbol{H}$) for an urban environment for typical mobile phone communication scenario [14]. The cross-polarisation discrimination is assumed to be 0 dB which is a typical value in mobile scenarios in for this multi-path environment.

The channel capacity is calculated for the proposed design at mode-2 at 950 MHz in Fig. 12*a*. The given figures show the channel capacity curves for the single-input–single-output (SISO) system, 2-element ideal MIMO antenna systems, proposed 4-element MIMO antenna system and 4-element ideal MIMO system in the urban mobile environment. It can be seen from the curves that the channel capacity curve of the proposed 4-element MIMO antenna system is less than the ideal 4-element MIMO antennas system but better than ideal 2-element MIMO antenna system and SISO system at SNR = 20 dB. The lower channel capacity curve of the proposed MIMO system is mainly because of the non-ideal efficiencies and non-zero correlation values. The ideal MIMO channel capacity curves are for uncorrelated channels and antennas system, which is practically impossible to achieve.

Cumulative distribution function (CDF) curves of the channel capacity for the given MIMO antennas are shown in Fig. 12*b* in an urban mobile environment. The advantage of the proposed MIMO antenna is evident.

4 Conclusions

In this paper, a compact isolation enhanced reconfigurable 4-element MIMO antenna system is presented. The proposed design is planar in structure and mostly suitable for small wireless handheld devices for CR applications. The reconfigurable dual-band, dual-mode antenna covers several frequency bands at lower-frequency bands below 1 GHz. The proposed MIMO antennas showed good bandwidth in all operating bands. Envelope correlation coefficient (ECC) evaluation based on the measured 3D radiation patterns of the antennas and channel capacity curves based on the 2D radiation patterns and a theoretical wireless channel showed a good MIMO performance metrics. The total space occupied by whole design was $65 \times 120 \times 1.56$ mm^3.

5 Acknowledgments

This project was funded by the National Plan for Science, Technology and Innovation (Maarifah) – King Abdulaziz City for Science and Technology – through the Science and Technology Unit at King Fahd University of Petroleum and Minerals (KFUPM) – the Kingdom of Saudi Arabia, under grant number 12-ELE3001-04.

6 References

1 Mansour, G., Hall, P.S., Gartner, P., *et al.*: 'Tunable slot-loaded patch antenna for cognitive radio'. Antennas and Propagation Conf. (LAPC), Loughborough, 2012, pp. 1–4
2 Cai, Y., Guo, Y.J., Bird, T.S.: 'A frequency reconfigurable printed Yagi-Uda dipole antenna for cognitive radio applications', *IEEE Trans. Antennas Propag.*, 2012, **60**, (6), pp. 2905–2912
3 Wu, T., Li, R.L., Eom, S.Y., *et al.*: 'Switchable quad-band antennas for cognitive radio base station applications', *IEEE Trans. Antennas Propag.*, 2010, **58**, (6), pp. 1468–1476

4 Hu, Z., Hall, P., Gardner, P.: 'Reconfigurable dipole-chassis antennas for small terminal MIMO applications', *Electron. Lett.*, 2011, **47**, (17), pp. 953–955
5 Lim, J.H., Jin, Z.J., Song, C.W., *et al.*: 'Simultaneous frequency and isolation reconfigurable MIMO PIFA using pin diodes', *IEEE Trans. Antennas Propag.*, 2012, **60**, (12), pp. 5939–5946
6 Chattha, H.T., Nasir, M., Abbasi, Q.H., *et al.*: 'Compact low profile dual port single wideband planar inverted-F MIMO antenna', *Antenna Wirel. Propag. Lett.*, 2013, **12**, pp. 1673–1675
7 Jain, A., Verma, P., Singh, V.: 'Performance analysis of PIFA based 4 × 4 MIMO antenna', *Electron. Lett.*, 2012, **48**, (9), pp. 474–475
8 Hussain, R., Sharawi, M.S.: 'A cognitive radio reconfigurable MIMO and sensing antenna system', *IEEE Antenna Wirel. Propag. Lett.*, 2015, **14**, (1), pp. 257–260
9 Tawk, Y., Christodoulou, C.: 'A new reconfigurable antenna design for cognitive radio', *IEEE Antennas Wirel. Propag. Lett.*, 2009, **8**, pp. 1378–1381
10 Tawk, Y., Costantine, J., Christodoulou, C.: 'Reconfigurable filtennas and MIMO in cognitive radio applications', *IEEE Trans. Antennas Propag.*, 2014, **62**, (3), pp. 1074–1084
11 Tawk, Y., Costantine, J., Avery, K., *et al.*: 'Implementation of a cognitive radio front-end using rotatable controlled reconfigurable antennas', *IEEE Trans. Antennas Propag.*, 2011, **59**, (5), pp. 1773–1778
12 Gobien, A.T.: 'Investigation of low profile antenna designs for use in hand-held radios'. Dissertation, Virginia Polytechnic Institute and State University, 1997
13 Sharawi, M.S.: 'Printed multi-band MIMO antenna systems and their performance metrics', *IEEE Antennas Propag. Mag.*, 2013, **55**, pp. 218–232
14 Gesbert, D., Shafi, M., Shiu, D., *et al.*: 'From theory to practice: an overview of MIMO space-time coded wireless systems', *IEEE J. Sel. Areas Commun.*, 2003, **21**, (3), pp. 281–302